

# NeuroSleepNet: A Multi-Head Self-Attention Based Automatic Sleep Scoring Scheme with Spatial and Multi-Scale Temporal Representation Learning

Muhammad Sudipto Siam Dip, *Member, IEEE*, Mohammad Abdul Motin, *Senior Member, IEEE*, Chandan Karmakar, *Senior Member, IEEE*, Thomas Penzel, *Fellow, IEEE*, Marimuthu Palaniswami, *Fellow, IEEE*

**Abstract— Objective:** Automatic sleep scoring is crucial for diagnosing sleep disorders. Existing frameworks based on Polysomnography often rely on long sequences of input signals to predict sleep stages, which can introduce complexity. Moreover, there is limited exploration of simplifying representation learning in sleep scoring methods.

**Methods:** In this study, we propose NeuroSleepNet, an automatic sleep scoring method designed to classify the current sleep stage using only the microevents in the current input signal, without the need for past inputs. Our model employs supervised spatial and multi-scale temporal context learning and incorporates a transformer encoder to enhance representation learning. Additionally, NeuroSleepNet is optimized for balanced performance across five sleep stages by introducing a logarithmic scale-based weighting technique as a loss function.

**Results:** NeuroSleepNet achieved similar and comparable performance with current state-of-the-art results. The best accuracy, macro-F1 score and Cohen’s kappa were 86.1%, 80.8%, 0.805 for Sleep-EDF expanded, 82.0%, 76.3%, 0.753 for MESA, 80.5%, 76.8% and 0.738 for Physio2018 and 86.7%, 80.9% and 0.804 for SHHS database.

**Conclusion:** NeuroSleepNet demonstrates that even with a focus on computational efficiency and a purely supervised learning approach, it is possible to achieve performance that is comparable to state-of-the-art methods.

**Significance:** Our study simplifies the automatic sleep scoring by focusing solely on microevents in the current input signal while maintaining remarkable performance. Therefore, this study offers a streamlined alternative for sleep diagnosis applications.

**Index Terms—** Electroencephalogram signal, multi-scale temporal context learning, sleep stage classification, spatial learning, transformer encoder, weighted loss function

## I. INTRODUCTION

Sleep is essential for human survival. Without adequate sleep, the body and mind cannot function properly. Also, the quality

of sleep patterns significantly influences both mental and physical well-being [1]. Understanding/Identifying sleep stages is crucial for medical treatment and diagnosis of various conditions such as sleep disorders, sleep apnea and psychiatric disorders [2]. The clinical sleep studies rely on Polysomnography signal (PSG) which consists of different biomedical signals such as Electroencephalogram (EEG), Electromyogram (EMG), Electrocardiogram (ECG) and Electrooculogram (EOG). Physicians and sleep experts collect these PSG data of a sleep subject and then analyze the signals over 20- or 30-seconds epochs to perform sleep scoring following the conventions outlined in Rechtschaffen and Kales (R&K) techniques [3], or the American Academy of Sleep Medicine (AASM) manual [4]. According to these guidelines, sleep stage is classified into wakefulness (W), rapid eye movement (REM), and three distinct non-REM (NREM) periods such as N1, N2 and N3. The occurrence of these stages varies overnight. A sleep expert may distinguish among these stages by their characteristics of distinct temporal and spectral patterns. Considering the AASM rule set, the presence of each of these stages can depend upon the transition rules or the sleep microevents such as slow-eye-movement, V-waves, arousal, K-complex, sleep spindles etc. However, hand-operated inspection of sleep stages requires efforts and a significant amount of time [5]. In contrast, automatic sleep scoring is time-efficient and requires minimal effort.

The sleep research field is experiencing a period of extraordinary progress in the development of automated sleep staging techniques. This is due to the growing number of available annotated sleep databases and increase in computational resources for processing large-scale datasets [6] [7]. The early studies of automatic sleep scoring involved the incorporation of hand-crafted features from various domains and use of traditional classifiers [8-12]. However, with the need of automating the learning of complex patterns into feature representation from the raw data and obtaining better performance, researchers have increasingly turned towards deep learning frameworks. Since the prior application of deep learning for classifying sleep stages, the efforts to contribute through diverse deep learning techniques can be categorized into two main areas. In earlier deep learning studies, many researchers used to extract handcrafted features before training a neural network-based classifier [13-18]. In subsequent research, numerous deep learning techniques were implemented to automate the feature extraction process,

Muhammad Sudipto Siam Dip and Mohammad Abdul Motin are with Department of Electrical & Electronic Engineering, Rajshahi University of Engineering and Technology, Bangladesh. (correspondence e-mail: m.a.motin@ieee.org).

Chandan Karmakar is with the School of Information Technology, Deakin University, Geelong, Victoria, Australia (karmakar@deakin.edu.au).

Thomas Penzel is with Interdisciplinary Sleep Medicine Centre, Charité University Hospital, Berlin, Germany (thomas.penzel@charite.de).

Marimuthu Palaniswami is with the department of Electrical & Electronic Engineering, The University of Melbourne, Victoria, Australia (palani@unimelb.edu.au).

thereby reducing the requirement for manual intervention [19] [20-22]. The recent studies have evolved towards designing end-to-end deep learning-based methodologies with effective network architecture. The Convolutional Neural Networks (CNNs) have proven to be a powerful tool for learning representations and integrating those with Fully Connected Neural Networks. (FCNNs) [16] [23]. Besides CNN-based architectures, Recurrent Neural Networks have been utilized due to their effectiveness with sequential data [24, 25]. Recently, hybrid model of CNN+RNN [26-31] has become very popular due to their ability to leverage the strengths of both CNNs in capturing spatial features and RNNs in handling temporal dependencies, making it highly effective. Other methods such as CNN+Transformer [32-35], transformer [36], image-representation based methodologies [37], joint representation [38] and transfer-learning [39, 40] are also explored in this field.

To get better EEG representation, architectures use feature maps with varied receptive field sizes for capturing different temporal and frequency patterns. For example, in [41], the authors proposed IITNet, that uses different convolutional filters to extract representative features from each segment and RNN for capturing the temporal theme of representative features. A similar study known as SleePyCo [34], the author used similar strategy of multiple convolutional blocks with different number of filters and used them together with a lateral mechanism to take the of benefits of multi-level features. However, both IITNet and SleePyCo depends on the previous adjacent epochs to make the following prediction. Filters with varying shapes a.k.a *multi-scale features* can be used to enhance the representation learning [32, 42]. According to [43], different filter shapes can capture different type of information in time-series data. For instance, to capture the temporal content of the data, filters with small shape works better while larger filters capture frequency components. The concept was utilized by A. Supratak et. al. in their DeepSleepNet model [26], which also employs Sequence model to account for the epoch-wise temporal information. However, their method includes multi-step learning and does not consider the intra-temporal content within a epoch. Later, this multi-scale approach has been examined in further studies on sleep by researchers such as [32, 42, 44], and [45]. However, direct extraction of multi-scale features from the signal often becomes more complex, requiring careful design and tuning of multiple scales. Furthermore, these methods may not effectively capture the spatial context (inter-channel relationships), especially when working with multivariate time series data.

Linear Spatial filtering techniques such as common spatial pattern, principal component analysis, or beamforming methods are useful for improving signal-to-noise ratio and reduce computational complexity [46, 47]. Deep learning based spatial filtering techniques has been in the first layer has been used [48, 49] to improve the representation of the input channels. S. Chambon et. al. [50] conducted a thorough investigation to measure the effect of a spatial filtering step on the enhancement of prediction performance. The study demonstrated that creating virtual channels using a CNN-based linear filter in the initial layer enhances model performance in subsequent stages that execute hierarchical feature representation. Yet, the use of spatial filters in conjunction with

other learning components remains uncharted. Moreover, their overall structure relies on analyzing both adjacent segments of the target segment to make predictions. A key advantage of previous studies with traditional methods is that hand-crafted features can be optimized to obtain very good performance with short sequence lengths. On the other hand, most of the deep learning methods use very large past epoch lengths and sometimes both past and future epochs to obtain similar results.

To overcome the above-mentioned constraints, we proposed NeuroSleepNet, that utilizes a spatial-temporal based feature extraction for automatic sleep scoring with only intra-epoch temporal context. Two layers of transformer encoder are used to transform general representations into more advanced and intricate representations. Four different datasets were used to investigate the performance of our model: SleepEDFx, MESA, PhysioNet2018, Sleep Heart Health Study (SHHS). The major contributions of our study are outlined below:

1. NeuroSleepNet incorporated the multi-scale temporal representation from the virtual channel output of convolutional spatial layer to make the later convolution operations easier and computationally efficient. The impact of the number of scales in temporal learning is also investigated in this research.
2. Most of the previous SOTA studies depend upon inter-epoch temporal context i.e.  $S > I$  where our primary goal was to utilize intra-epoch context by using only current epoch (one-to-one) while providing comparable performance of many-to-one approaches. The benefit of this is our model can classify a sleep stage without looking the previous or next stage. Thus, the dependency of using transition rules to take into account for automatic scoring is reduced.
3. We derived a method for adjusting feature representations in order to use them into multi-head encoder network in a more suitable manner and receive more refined representation.
4. We incorporated a logarithmic-scaled weighted function into our loss function to address class imbalance in sleep databases and achieve more balanced results.
5. We validated the NeuroSleepNet model using four publicly available datasets. Our findings demonstrate that NeuroSleepNet achieves comparable performance and exceeds that of most state-of-the-art studies reported in the literature.

## II. NEUROSLLEEPNET

### A. Design Principles

#### 1) Statement 1: Input type and generalization

From the available PSG signals, our study aimed to design a neural network-based architecture that can take both multi-channel and single-channel-based input. The single channel follows more concise architecture than that of multi-channel. In our single-channel experiments, the initial block is neutralized while the remainder of the network remains active. Deep learning networks have a voracious appetite for more data. More data improves the generalization capability. Although with increasing data, the model needs to be optimized. For example, if the number of training data is large, the network capacity should be increased to mitigate lower learning

capacity. Thus, an aim is to design the network in such that can provide firm performance regardless the amount of training data without changing the model parameters.

### 2) Statement 2: Addressing Class Imbalance Problem

*NeuroSleepNet trained such that the class imbalance problem is reduced and balanced accuracy is also improves with general accuracy*

Five distinct stages occur with significant diversity throughout the night. A model can forecast the labels based on the quantity of samples it includes. For instance, the appearance of N2 happens more rapidly during sleep compared to N1. For example, if N2 represents 60% of the training data, it is probable that the model will exhibit better performance with N2 and relatively poorer performance with N1 because N1 occurs rarely. Using the same concept, the accuracy can be increased by introducing more data in the Wake (W) class, before and after the total sleep duration. Furthermore, N1 stage and REM stage have a chance to have higher misclassification between each other since these stages share almost similar characteristics. Thus, an overall accuracy does not truly reflect the actual performance of the model. To avoid this, a model should be designed such that it not only increases the accuracy but also does a trade-off with other parameters such as MF1 and balanced accuracy. In our study, we computed both overall accuracy and balanced accuracy as the main metrics to evaluate the performance of our model. To tackle the imbalance nature of the dataset and reduce its impact on the performance we proposed a logarithmic scaled weight assignment strategy for the cost function outlined in section II-E.

### 3) Statement 3: Problem statement

**Standard Formulation (one-to-one):** The dataset is constructed with  $n$  number of 30s EEG segments sampled at 100Hz. Here,  $X = \{x_1, x_2, \dots, x_n\}$  represents the  $n$  number of EEG segments in which  $x_i = \mathbb{R}^{C \times T}$ . The  $C$  represents the number of channels and  $T$  is the total samples per segment. Corresponding to  $x_i$ , the label is defined as  $y_i \in \{0, 1\}^Y$  where  $Y=5$ , indicates the set of five stages of sleep notably {W, N1, N2, N3, R}. In our standard one-to-one approach, the NeuroSleepNet takes only the current segment  $x_i$  to predict its corresponding label  $y_i$ .

**Successive Epoch Length (many-to-one):** Apart from standard formulation of one-to-one method, NeuroSleepNet is also constructed to experiment how much the previous segments impacts the performance of the current segment to compare those results with our primary one-to-one implementation. For our many-to-one experiment, our model takes an input of  $X_S = \{x_1, x_2, \dots, x_S\}$  such that  $X_S \in \mathbb{R}^{C \times T \times S}$  and the sequence length is set such that  $1 < S \leq 5$ . Here,  $S$  is the sequence length,  $x_S$  is the target segment and  $y_S$  is the sleep stage label of target segment. In this many-to-one experiment, although the model takes  $S-1$  numbers of previous segments to predict the target segment  $y_S$ .

### B. Convolutional Spatial Filtering

The spatial concept in this paper was inspired by [50] which shares similar motivation of previous studies mentioned in [48] [49]. Here, the aim is to create a convolutional block that can process simultaneously at each time point, rather than working independently on each channel. The advantage of this is allowing the model to learn cross-channel features that facilitate subsequent analysis. The convolution block carries out a linear

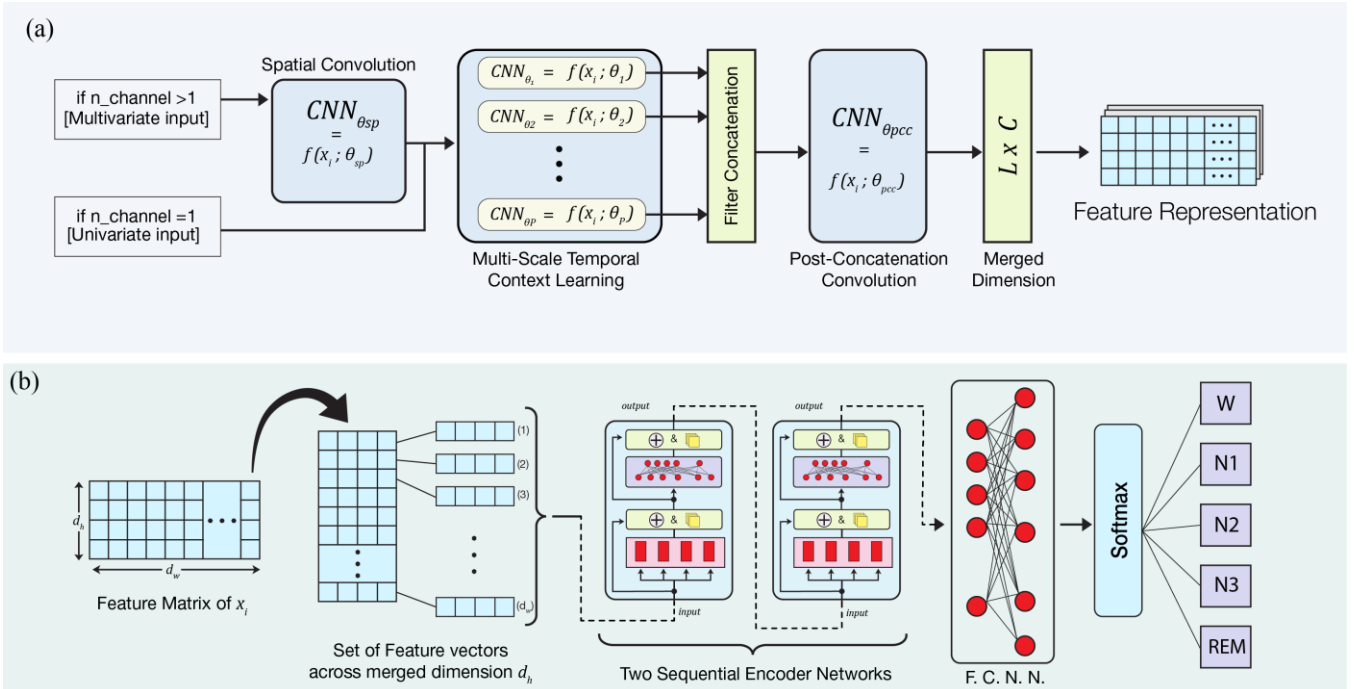


Fig. 1: The model architecture of NeuroSleepNet consist of a) Representation learning to extract features with the help of spatial and multi-scale temporal context learning which then concatenated across the filter dimension followed by post concatenation convolution block. Lastly, the filter and additional channel dimension is merged b) Refining feature representations from static to contextual features and passing them into a shallow fully connected neural network classifier.

operation on the multi-channel input, generating virtual channels that represent the input channels. Spatial filtering was performed using a 2D convolutional block with filters equal in number to the input channels and a kernel size of  $(C, 1)$ . The output from this block was permuted to get into the original shape. The resulting outputs were two vectors representing two channels and have the same input length  $T$  as the raw input. Formally, since we are using 2D convolution, it takes a 2D input of  $(1, C, T)$  reshaped from  $(C, T)$ , where  $C$  is the number of channels indicating input height  $h_i$  and  $T$  is samples per segment indicating the width of the input  $w_i$ . Since, the filter size is  $(\kappa_h, \kappa_w) = (C, 1)$ , we can indicate the stride height  $h_s$  is equal to 1 and the stride width  $w_s$  is equal to 1. Thus the output height,

$$h_{sp} = \frac{h_i - \kappa_h}{h_s} + 1 \quad (1)$$

which is equal to 1 and output width,

$$w_{sp} = \frac{w_i - \kappa_w}{w_s} + 1 \quad (2)$$

which is equal to  $T$ . Therefore, combining every channel the output is  $(1, T)$  and since the number of filter is same as the number of channel  $C$ , we get the final output of the spatial block as  $(|B|, C, 1, T)$ , where  $|B|$  is the input batch size. The output is permuted back to  $(|B|, 1, C, T)$  to get back to its original input shape for later processing.

### C. Multi-Scale Temporal Context Learning

NeuroSleepNet employs convolutional blocks of various scales simultaneously to extract the temporal context from the virtual input channels known as multi-scale temporal context learning (MTCL). We denote the number of convolutional blocks in parallel as  $P$ . Each block includes several convolutional filters, a rectified linear unit (ReLU) for activation, and a max-pooling layer to down-sample the CNN outputs. The total CNN operation can be shown as

$$CNN_{MTCL} = \{CNN_{\theta_1}(\cdot), \dots, CNN_{\theta_P}(\cdot)\} \quad (3)$$

Here,  $\theta_j$  represents the parameter of  $j^{\text{th}}$  CNN indicating its distinct filter size. From the feature matrix created as virtual channels  $X'$ , the MTCL takes  $x_i'$  and outputs a series of feature arrays denoted as

$$C_{t,i} = \{C_t^{\theta_1}, C_t^{\theta_2} \dots C_t^{\theta_P}\} \quad (4)$$

Considering CNN 2D as temporal convolution with kernel size  $(\kappa_h, \kappa_w)$  is set as  $(1, K)$  and the number of filter  $L$ , each CNN block outputs  $L$  number of feature matrices shaped  $(h_{mtcl}, w_{mtcl})$ . A regular 1D CNN takes a single batch with an input shape of  $(C, T)$ . But since we are using 2D CNN, every batch was reshaped into  $(1, C, T)$  in the previous stage which includes an additional dimension of 1 that can be considered as the channel dimension that treats the signal similar to a greyscale image which has the channel dimension or color channel of 1. The strategy is to keep the dimension of EEG channels,  $C$  same as we apply convolutional filters across additional channel dimension.

The kernel width  $K$  is taken differently for different blocks in the MTCL operation, described in III-C.

$$h_{mtcl} = \left[ \frac{h_i - \kappa_h + 2 \times p}{h_s} + 1 \right] \quad (5)$$

which is equal to  $C$  as padding  $p$  is 0, and

$$w_{mtcl} = \left[ \frac{w_i - \kappa_w + 2 \times p}{w_s} + 1 \right] \quad (6)$$

which is kept as same length as  $T$  by adjusting the padding size as

$$p = \frac{\kappa_w}{2} = \frac{K}{2}. \quad (7)$$

Each of the convolutional block in MTCL down-samples with a max-pooling layer having a pools from  $r$  temporal samples. Thus, every feature array  $C_t^{\theta_j} \in \mathbb{R}^{L \times C \times [T/r]}$ . Each of the parameters are depicted in Table II of the paper. Following the MTCL, we performed filter concatenation ( $\oplus$ ) to the each output of  $C_t$  across the dimension of filter that can be denoted as

$$C_{t(cat),i} = [C_t^{\theta_1} || C_t^{\theta_2} || \dots || C_t^{\theta_P}]_{dim=1} \quad (8)$$

The number of filters after filter concatenation is  $L' = P \times L$ . Thus, the concatenated array is  $C_{t(cat),i} \in \mathbb{R}^{(L \cdot P) \times C \times [T/r]}$ . This concatenated array is passed to a post-concatenation convolution (PCC) block with ReLU activation and a max-pooling layer and to simplify the combined representations coming out of the MTCL. The parameters of this convolutional block is kept similar to the first convolutional block of MTCL denoted as  $CNN_{\theta_1}(\cdot)$  which had the smallest filter scale among all. The output of this PCC is  $C_{PCC,i} \in \mathbb{R}^{L \times C \times [T/(r \cdot r)]}$ . The benefit of this operation is further discussed in the discussion section. The filter dimension and channel dimension is merged into a single dimension by multiplying them and result denoted as  $C_{out,i} \in \mathbb{R}^{(L \cdot C) \times [T/(r \cdot r)]}$  where  $C_{out,i}$  represents final feature matrix of  $i^{\text{th}}$  segment from the mini-batch in our representation learning. The output from here is permuted again and prepared for the transformer encoder layer. The overall steps for representation learning are simplified in Fig. 1(a).

### D. Self-Attention Based Multi-Head Encoder

To generate more complex and higher level representation of extracted features from representation learning, we employed multi-head self-attention based transformer. In NeuroSleepNet, we used the encoder part from the original study [51]. A self-attention network is capable to convert static features into contextual features depending on the adjacent sequences while multi-head mechanism in self-attention can capture multiple perspective of the input representations. Fig. 2 provides a simplified illustration of the transformer encoder mechanism used in our model. The parameters in NeuroSleepNet are modified from the original architecture. In this study, we only used  $N = 2$  identical encoders sequentially. Each encoder is consist of  $n_{head} = 4$  i.e. four self-attention blocks. The encoder takes a feature matrix of  $C_{out} \in \mathbb{R}^{d_h \times d_w}$  where  $d_h = (L \cdot C)$  represents merged dimensions of filters and EEG channels and  $d_w = [T/(r \cdot r)]$  represents pooled temporal sequence length, denoted for simplification for the later stages. The input of encoder network takes  $d_w$  number of sequences or vectors where each vector is consist of  $d_h$  values/points. The input of encoder network can be easily related to that of natural language processing in which, we can consider  $d_w$  as number of word embedding vectors where each one is consist of  $d_h$  number of values representing  $d_h$  distinct characters. Thus,  $d_h$  is considered the shape of  $d_{model}$  a.k.a. embedding dimension of the transformer encoder. Fig. 1(b) shows simplified representation of data arrangement for the transformer encoder and the following steps.

The following of four self-attention block is addition operation with the original input sequence and layer normalization is followed as the original settings. The second part of the encoder network uses a default two layered feed-forward neural network where the hidden layer consists of  $\text{dim\_feedforward} = 2048$  units with ReLU activation function and a dropout of 0.25. The following layers outputs a series of vectors where each vector has  $d_{model}$  number of values for each input sequence. Formally, it can be written as,  $\mathbf{z} = \{z_1, z_2, \dots, z_n\}$ . The output is then again added with the previous inputs i.e. the normalized vectors and normalized again with 2<sup>nd</sup> layer normalization. The final output can be depicted as

$$\mathbf{y} = \text{TransformerEncoder}(C_{out,i}, \theta_e) \quad (9)$$

Where  $\mathbf{y} = \{y_1, y_2, \dots, y_n\}$  and  $\mathbf{y} \in \mathbb{R}^{d_h \times d_w}$  indicates the same shape of the input of transformer encoder. The output  $\mathbf{y}$  is then flattened by averaging across their temporal dimension  $d_w$  using the following relation:

$$A_i = \frac{1}{d_w} \sum_{j=1}^{d_w} d_{h_j} \quad (10)$$

Where,  $A_i \in \mathbb{R}^{1 \times d_h}$ . This flatten-out vector representing  $i^{\text{th}}$  segment from a mini-batch is fed to a single layered neural network classifier and a softmax function. Most of the previous automatic sleep scoring studies were heavily influenced by RNN based methods because of their capability of capturing transitional changes in sequence data. Since the self-attention-based architecture is a non-recurrent mechanism, a method called positional encoding is applied to the input of the encoder. However, in our study the positional encodings were not included with the input features of the encoder network. Finally, the processed feature representations are fed into a single layered neural network layer with  $L \times C$  number of hidden units followed by a softmax layer to predict the sleep stage.

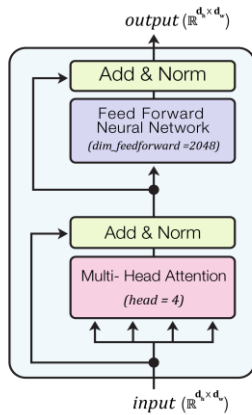


Fig 2: Simple architecture for multi-head self-attention encoder network.

### E. Log-Scaled Weighted Cost Function

The cross-entropy loss for a multi-class classification task is a loss function to measure the performance of a classification model. It measures the discrepancy between the actual probability distribution found by a classification model and the predicted values. In a conventional way, the cross-entropy loss is computed from a mini-batch of data containing  $n$  segments; the model predicts the output logits shaped  $(n, Y)$ . Each of these logits are then converted into probabilities with this softmax expression:

$$p_{i,Y} = \frac{\exp(x_{i,Y})}{\sum_{j=1}^Y \exp(x_{i,j})} \quad (11)$$

Where  $i$  indicates sample index and  $Y$  is the number of classes. From the matrix of probabilities, at each sample, the probability corresponding to the true class  $y_n$  is selected to calculate the individual loss of the sample as given:

$$l_i = -\log(p_{i,y_n}) = -\log \left\{ \frac{\exp(x_{i,y_n})}{\sum_{j=1}^C \exp(x_{i,j})} \right\} \quad (12)$$

For the total  $n$  number of samples in a mini-batch, the individual loss is computed for all the samples as a vector  $\ell(x, y) = \{l_1, l_2, \dots, l_n\}^T$  from which the individual losses are used in a combination technique (e.g. mean, median etc.) to calculate the representation of the overall loss,  $\mathcal{L}$  of the mini-batch.

In our research, we included a class weight technique that computes regular class weights and applies a logarithmic scaling to those weights before multiplying them with the actual loss function. The scaled weights provide an optimized penalty to the minority class if misclassification occurs. The regular class weight calculation of a class is inversely proportional to the class frequency of that class, calculated by  $\frac{\sum n}{f_{y_i}}$ . Now, this

weight calculation technique can result in high variance weights among the classes and assigns very low weights for the class with sufficient data while assigning very large weight for the class with a very few samples. This can lead to reduce the individual performance of a class even though it has sufficient training data. To solve this issue we applied a logarithmic transformation to this weight calculation method which is:

$$w_{y_i} = \log \left( \frac{\sum n}{f_{y_i}} \right) \quad (13)$$

Thus reducing the range in the scale while keeping the comparative differences. Multiplying it with the original cross-entropy loss of individual samples implies,

$$l'_i = -\log \left( \frac{\sum n}{f_{y_i}} \right) \cdot \log \left\{ \frac{\exp(x_{i,y_n})}{\sum_{j=1}^C \exp(x_{i,j})} \right\} \quad (14)$$

To calculate the overall loss, we normalize the individual losses in the modified set of losses. Finally, we get our modified loss function as:

$$\mathcal{L}' = \frac{1}{n} \sum_1^n -\log \left( \frac{\sum n}{f_{y_i}} \right) \cdot \log \left\{ \frac{\exp(x_{i,y_n})}{\sum_{j=1}^C \exp(x_{i,j})} \right\} \quad (15)$$

## III. EXPERIMENTS

### A. Datasets

In our experiment, we used four public datasets on automatic sleep scoring. These involves: Sleep-EDF Database from PhysioNet, MESA dataset from NCSR, Sleep Heart Health Study from NCSR and Physonet2018 database. The overall summary and splitting ratio of these sleep dataset is shown in Table I. We employed Sleep-EDF database as our primary source of various experiments and also utilized the other databases to obtain the performances.

TABLE I  
DATASET DESCRIPTION AND EXPERIMENTAL SETUP

Ind	Name	No. of Recordings	Channels	Scoring	Validation Set	Test Set
1	Sleep-EDF	78	Fpz-Cz, Pz-Oz	R&K	0.02% of training data	7 Subjects
2	MESA	2237	C4-M1, Oz-Cz, Fz-Cz	AASM	0.05% of training data	20 Subjects

3	Physio 2018	994	F3-M2, F4-M1, C3-M2, C4-M1, O1M2*, O2-M1*	AASM	0.04% of training data	20 Subjects
4	SHHS	5791	C3-A2, C4-A1	R&K	0.04% of training data	25 Subjects

\* Indicates the channels that were excluded during the preprocessing.

### 1) Sleep-EDF Expanded

The sleep-EDF expanded database is one of the most popular datasets in automatic sleep scoring studies [52, 53]. The dataset is accessible in PhysioNet's databases [54]. The scoring method in the Sleep-EDFx database used was R&K techniques [3]. The dataset consists of two EEG channels: Fpz-Cz and Pz-Oz, a horizontal EOG, a submental chin EMG, and an event marker. There are 197 whole night PSG recordings divided into two types. The first 153 sleep recordings known as *Sleep Cassette (ST)* were recorded from 78 healthy Caucasians between age of 25-101, without any sleep medications. Among the 78 subjects, 75 had recordings from two nights, 2 subjects had recordings only from the first night, and 1 subject had a recording only from the second night. This resulted in a total of 153 recordings. The Sleep Telemetry has 44 sleep recordings from 22 Caucasian males and females with temazepam effects on sleep. These subjects experienced slight difficulty falling asleep. In our study we only used the *Sleep Cassette* recordings. In ST, the EEG and EOG signals had sampling frequency of 100Hz, and EMG was sampled at 1Hz. The sleep recordings and the sleep annotations, both were given in EDF format.

### 2) Multi-Ethnic Study of Atherosclerosis

Multi-Ethnic Study of Atherosclerosis (MESA) [55] [56] is a set of PSG recordings that included 2237 sleep participants of different ethnicity such as white, Caucasian, Chinese American, Black, African American and Hispanic. 1198 subjects were female, while 1039 were male. The participants were between the ages of 54-95. The EDF files contain 27 biosignal channels

from which there are three EEG channels (central C4-M1, occipital Oz-Cz, and frontal Fz-Cz leads) were used to record the brain activity during sleep. The sleep annotations were given in the XML annotation files given as profusion. The sleep annotations were scored over 30 seconds of sleep segments following the AASM manual of sleep scoring [4]. The EEG signals were recorded with a sampling frequency of 256Hz.

### 3) Sleep Heart Health Study

The National Heart Lung & Blood Institute conducted the Sleep Heart Health Study (SHHS) to investigate the effect of sleep-disordered breathing on heart diseases [55] [57]. The sleep recordings of SHHS are divided into two datasets following their timeline. The SHHS consists of PSG recordings belong to 5791 participants. All participants aged 40 or older have no prior history of sleep apnea treatment. The PSG contains two recordings of two EEG channels namely C3/A2 and C4/A1, each sampled at 125 Hz. It also includes two EOG (R and L), sampled at 50Hz and a bipolar submental EMG, sampled at 125Hz. The manual sleep scoring was done by following the R&K guidelines [3].

### 4) PhysioNet2018

The dataset for PhysioNet challenge 2018 was contributed by Massachusetts General Hospital [58] [54]. The dataset consists of 1986 subjects total in which 994 subject's recordings were provide to develop and train a sleep scoring system to detect sleep arousal (non-apnea) during sleep. 67% of the available train dataset contains male subjects and the other 33% were female. The average age of the subject is 55 with a standard deviation of 14.3. The dataset contains various physiological signals such as EEG, EOG, EMG, ECG, SaO2. There were six EEG channels used at F3-M2, F4-M1, C3-M2, C4-M1, O1-M2, and O2-M1 based on the International 10/20 System. The signals were recorded with a sampling frequency of 200Hz. The sleep experts used the AASM standards [4] to do manual scoring.

TABLE II  
MODEL SPECIFICATION OF NEUROSLLEEPNET'S REPRESENTATION LEARNING. THE FEATURE EXTRACTOR IS DIVIDED INTO THREE STAGES 1) SPATIAL LAYER 2) MTCL AND 3) PCC

LAYER NAME	LAYER TYPE	FILTER S(L)	FILTER SIZE	STRIDE	OUTPUT SHAPE	ACTIVATIONS	PADDINGS
SPATIAL LAYER	Input	--	--	--	(C, T)	--	--
	Reshape	--	--	--	(1, C, T)	--	--
	Conv 2D	C	(C, 1)	(1, 1)	(C, 1, T)	Linear	--
Permute	--	--	--	--	--	--	--
MTCL	Conv2D	8	(1, $K_1 \times i$ )	(1, 1)	(8, C, T)	ReLU	$K_1/2$
	Maxpooling 2D (i=1)	...	(1, 12)	...	(8, C, T//12)	...	...
	...	...	(1, $K_P = K_1 \times P$ )	...	(8, C, T)	ReLU	$K_P/2$
	Conv2D	8	(1, 12)	(1, 1)	(8, C, T)	ReLU	$K_P/2$
Filter Concatenation	--	--	--	(8*P, T//12)	--	--	--
PCC	Conv 2D	8	(1, $K_1 \times i$ )	(1, 1)	(C, 1, T)	ReLU	$K_1/2$
	Maxpooling 2D	--	(1, 12)	--	--	--	--
	Dimension Fusion	--	--	--	(8*C, T//(12*12))	--	--
	Permute	--	--	--	(T//(12*12), 8*C)	--	--
	Permute	--	--	--	--	--	--

## B. Preprocessing & Data Preparation

Most EEG information is concentrated in the lower frequency regions of the signal [59]. The lower frequency ranges typically divided into several bandwidth where a sleep stage may occur under a specific bandwidth. For example, the signal in the frequency range of (0.5-4 Hz) *a.k.a.* delta wave represents deep sleep while mu-wave which occurs in the range of (8-13 Hz) represents wakefulness. We used a 0.5Hz to 30Hz band-pass filter to remove signal components from higher frequency bands unrelated to sleep stages. Then 30 second epochs were created and sleep annotations were included with each epoch. In the primary experiment data, sleep-EDFx, we included 20 minutes of wake data before sleep, but none after the total sleep duration. For other datasets, we did not include any data outside of the actual sleep period. All datasets, except Sleep-EDFx, were downsampled to 100Hz to match the sampling frequency of Sleep-EDFx since NeuroSleepNet was optimized with this dataset. While creating sleep segments a data normalization technique known as standard scalar was applied to the EEG data. For standard one-to-one experiment, the epoch is  $x_i = \mathbb{R}^{C \times T}$  where the  $T$  indicates time-step of one epoch. For the implementation of Successive Epoch Length (many-to-one), the length of each epoch is  $C \times T \times S$ .

## C. Model Specification

The feature extractor part to extract representation from the signal is divided into three stages. The smallest scale i.e. filter size in the convolution block in MTCL was  $K=0.25$  seconds that processes  $K * f_s = 0.25 * 100 = 25$  samples at once and slides with a stride of 1. The scale size of  $i^{\text{th}}$  block is set as  $i * K$  that results in  $K = \{25, 50, 100 \dots\}$ . The number of convolutional blocks ( $P$ ) was determined by a thorough experiment of employing  $P$  from 1 to 5. The best number of parallel scales were set to  $P=3$ . The details is outlined in section IV-C. Previously, it was stated that, small filter can learn temporal context while larger one can learn frequency content of the time-series data. For sleep stage classification, however, it is hard to determine the exact filter size and combination in which this goal is perfectly achieved. Therefore, in our experiment, we investigated by sequential inclusion of convolutional blocks in MTCL, each time with the twice the scale size of previous added block. The results are shown in Fig. 7 for each dataset. The same filter cannot extract the same information from different dataset if the sampling rate during signal acquisition is different. Thus, during preprocessing, downsampling was applied to convert those signals that has higher sampling rate to make them similar to our primary experimental dataset Sleep-EDF. Therefore, the  $T$  was 3000 for all the dataset used in our study. To utilize different dataset with different  $f_s$  with appropriate  $P$  and scales  $K$ , further studies are required. The number of temporal values that were max-pooled were set to  $r=12$  for all the post convolutional operation. And the output logits were not normalized and taken as they were from each blocks. Our model uses ADAM optimizer with a learning rate of  $lr = 1e-3$  and weight decay regularization with a value of  $\gamma = 1e-3$ . For all the dataset, the model was trained with a fixed training batch-size of 512 and validated during training with a batch-size of 256. The total number of parameters in

NeuroSleepNet for our multivariate scheme was  $2.18 \times 10^5$  and for univariate scheme it was  $1.17 \times 10^5$ .

## D. Experimental Design and Evaluation Scheme

We assessed our model using a hold-out test set specified in Table I for each dataset. The test set is chosen differently for different datasets and were kept separate from training and validation set. During the training, the evaluations were made with a k-fold cross validation method. For sleep-EDFx dataset, the k was set to 20. For each fold, n/20 subjects' data were used to validate the model while the rest of the  $n(k-1)/k$  data were used to train the model. For other datasets, the split for train-validation and test are also shown in Table I. After the training, the final model is evaluated with the hold-out test set. The evaluation metrics we used in our study includes, accuracy, macro-F1 score, and Cohen-kappa score. We also showed the confusion matrix for five-class classification to represent how much our model performs for each task with per-class recall scores. To measure the fraction of correctly classified sleep stages out of all five classes, we calculated accuracy while balance accuracy was calculated to account for class imbalance issue by averaging recall score for each stage of sleep.

$$Accuracy = \frac{\sum_{i=1}^Y TP_i}{n} \quad (16)$$

$$Balanced Accuracy = \frac{1}{Y} \sum_{i=1}^Y \frac{TP_i}{TP_i + FN_i} \quad (17)$$

Where  $TP_i$  is the true positive for class  $i$ ,  $FN_i$  is the false negative for class  $i$ , and  $n$  is the total number of instances. The macro F1-score measures the harmonic mean of precision, and recall, averaged across classes.

$$F1 - Score (Macro) = \frac{1}{Y} \sum_{i=1}^Y F1_i \quad (18)$$

Where  $F1_i$  is the per class F1-score defined as  $F1_i = 2 \times \frac{Precision_i \times Recall_i}{Precision_i + Recall_i}$

Finally, we calculated Cohen's Kappa coefficient with the following equation:

$$\kappa = \frac{p_o - p_e}{1 - p_e},$$

Where the observed agreement,  $p_o$  is calculated with,  $p_o = \frac{1}{n} \sum_{i=1}^Y TP_i$  and the expected agreement  $p_e$  is  $p_e = \frac{\sum_{i=1}^Y ((TP_i + FP_i) \times (TP_i + FN_i))}{n^2}$

## IV. RESULTS AND DISCUSSIONS

NeuroSleepNet model was examined using four publicly available datasets mentioned earlier. The results are shown in IV-A. The rest of the subsections are many additional experiments that were utilized by our primary dataset Sleep-EDFx.

### A. Performance Comparison with Previous State-of-the-art models

The performance of NeuroSleepNet is shown in table III and compared with the existing state-of-the-art (SOTA) models for automated sleep scoring. The performance metrics used in the comparison are accuracy, micro-F1 score, Cohen-kappa value and per-class F1 score. The performance of the model measured in balanced accuracy, macro-precision and macro-recall scores are given in Table III. In the comparison, we included the frameworks of SOTA models, input type, sequence length (S) simultaneously. The table displays the superior results of our approach compared to other methods. The confusion matrix on NeuroSleepNet model for one-to-one approach is shown in Fig.

3 for Sleep-EDF, MESA, PhysioNet2018 and SHHS datasets. Furthermore, a hypnogram plot comparing the model's predictions with the annotations scored by a human sleep expert is also presented in Fig 4. In our one-to-one approach, the overall accuracy, MF1 score, and Cohen-kappa value is 86.7, 80.8, 0.805 for Sleep-EDF, 82.0 76.3 0.753 for MESA, 80.5, 76.8, 0.738 for Physio2018 and 86.7, 80.9, 0.804 for SHHS dataset. Our model achieved superior or almost similar to the existing SOTA performance by incorporating MTCL with spatial convolution and using transformer encoder to convert the initial representation into higher level representation. The spatial layer makes it easier to learn the temporal features in multiple scale for convolutional blocks in MTCL. Moreover, our multi-head attention network captures multiple perspective of a same representation. Thus, helping the network to learn from those representations with diverse temporal and frequency scales. The confusion matrices and table show that without changing the model's parameters the model provides robust performance for different dataset distinct in size and characteristics. This satisfies one of our design principles outlined in statement 1 of II-A.

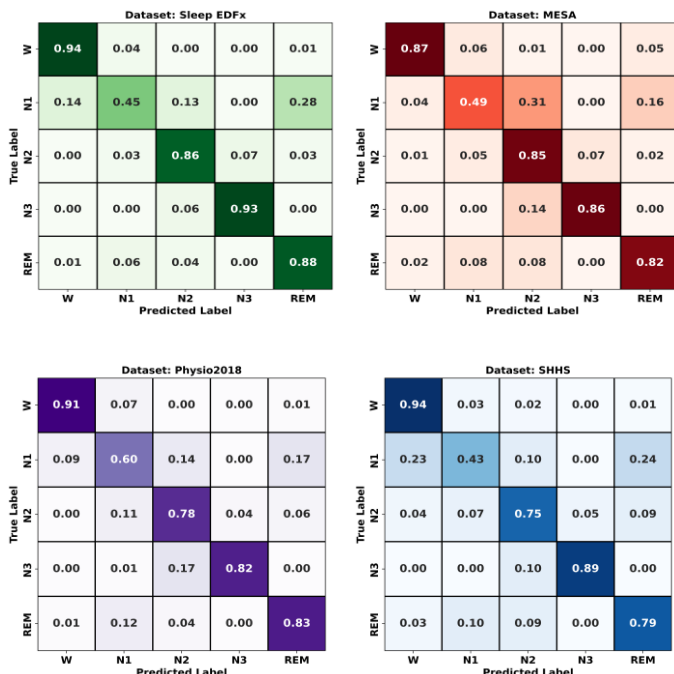


Fig 3: Confusion matrix of NeuroSleepNet on four datasets: Sleep-EDF, MESA, Physio2018 and SHHS. We converted the output values in per-class recall scores. AC indicated the actual class positioned vertically and PC represents predicted class positioned horizontally.

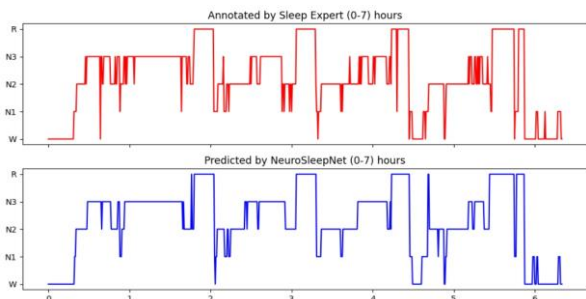


Fig. 4: Two hypnogram comparing the performance of sleep scoring by a human expert and NeuroSleepNet. The comparison is done on the recordings

of subject 01 from Sleep-EDF dataset. For this subject the scores are acc: 86.4, Mf1: 81.3, and  $\kappa$ :81.9.

The major advantages of NeuroSleepNet, in comparison to other SOTA model is achieving great performance with single input epoch while reducing computation complexity. Our model can be utilized in both single channel and multi-channel scheme and can achieve comparable performance by employing raw signal with minimal preprocessing i.e. filtering. However, the proposed method does not require any need for hand-crafted features nor time-frequency image representation of the raw signal. The existing SOTA is based on multi-view scheme that uses both raw signal and time-frequency image as their input [38]. In automatic sleep scoring, one cannot argue that utilizing time-frequency representation is better than using raw signal alone since there are various considerations. In contrast, our proposed method is designed to achieve comparable SOTA performance with only raw signal. The other methods that achieved SOTA performance with raw signals either requires higher number of input epochs compared to ours [34] or requires both previous and subsequent sleep segments [50]. Although, NeuroSleepNet demonstrated comparable performance using only with single epoch, it can achieve greater performance with smaller number of input epoch compare the existing models. The one-to-one approach is more feasible and realistic for the implementation of clinical sleep scoring. Creating virtual channels through spatial convolution can potentially be applied to various classification tasks and other signal applications.

### B. NeuroSleepNet Optimizes Balanced Performance

It has been mentioned earlier that for a highly imbalanced dataset measuring the metric accuracy does not represents the overall performance accurately. Thus, in this section we measured the balanced accuracy of NeuroSleepNet on all four dataset and compared with regular accuracy. The comparison is shown in Fig 5. The comparison demonstrates the minimal difference in accuracy and balanced accuracy. Therefore, depicting that NeuroSleepNet to be a more robust model. Also the minimal difference in those two parameters also supports our claim outlined in 2<sup>nd</sup> design principle in II-A. Furthermore, The balanced accuracies of baseline models compared with our NeuroSleepNet model for both univariate and multivariate cases using the Sleep-EDF dataset shown in Fig 6. The comparison indicates that the balanced performance for the univariate input with the Fz-Cz channel closely resembles that of H. Korkalainen et al. [30], XSleepNet [38], and SleepPyCo [34]. For multivariate input, the balanced performance is higher than all other baseline models. The multivariate input includes the Pz-Cz channel as its input with the primary Fpz-Cz channel, where both channels are processed into a virtual channel with a spatial convolution operation. The measurement suggests that signals acquired from the parietal region of the brain using the primary frontal channel can improve balanced performance significantly.



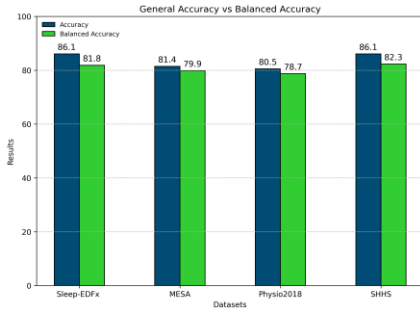


Fig. 5: The comparison between overall accuracy and balanced accuracy for all four datasets. The comparison indicates that both the accuracy and balanced accuracy are close to each other thus indicating NeuroSleepNet’s robustness on scoring all five classes.

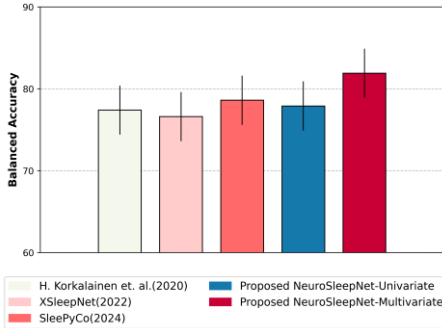


Fig. 6: Balanced accuracy comparison between baseline models and the proposed NeuroSleepNet model (univariate & multivariate).

### C. Number of Scales in MTCL and Post Concatenation Convolution

The number of scales in the MTCL stage was determined by evaluating  $P$  from 1 to 5. Fig. 7 presents the results for various number of scales, showcasing accuracy, macro-f1 score and kappa score on Sleep-EDFx. The smallest scale accounts 0.25 seconds of data. Thus, the smallest scale was 25 since the sampling frequency was 100Hz. With the inclusion of each block in MTCL, the scale size was taken twice as the size of previous block. The results shows that the performance increases with inclusion of new block and at  $P=3$ , the model provides best performance. However, after the inclusion of 3rd block the performance decreases. We assumed since we were using a PCC layer following the MTCL stage to make a combined representation, the PCC’s ability to combine the representation of MTCL decreases for too many scales and in our case the threshold was 3. The motivation behind PCC was same as lateral connection following a backbone network. A lateral connection can create identical representation from the outputs from different blocks (feature pyramid) in the backbone containing various number of filters and kernel sizes. On the other hand, PCC first combines the outputs prior and creates a single representation that will represents the output all the previous blocks in a combined feature matrix. However, if the filter concatenation has to combine too many blocks in previous layer, the individual sequences that represents a MTCL block reduces. Also, a very small or a very large scale in a convolution can create redundant information based on the characteristics of the signal. Conversely, if PCC block was not used not only it would fail to integrate different perspective in a single

representation but also the sequence length would have been larger. The max-pooling in PCC reduces the sequence from  $L \times C \times [T/(r.r)]$  to  $L \times C \times [T/r]$ . Without the PCC, the Eq. (10) would have to compute the average from a temporal sequence  $r$  time larger than the output of PCC. Thus, the overall representation of the architecture before dense layered classifier would contain mean values that stabilizes around zero leading to a poorer representation.

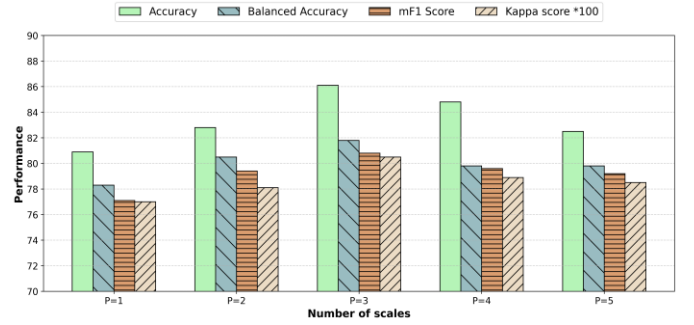


Fig. 7: The performance comparison for different number of scales ( $P$ ) from 1 to 5, measured in accuracy and balanced accuracy. The overall best value of  $P$  is 3 and used in final architecture of NeuroSleepNet.

### D. Weighted cost function compared with other conventional weighted approaches.

There are different ways of addressing the class imbalance problem. The impact of class imbalance problem is severe and reduce the learning capability of the classes with a smaller number of samples. One of the major methods of dealing with class imbalance problem is data augmentation. Data augmentation is a process of artificially increasing the size of the dataset by including more samples, by applying different transformation to the existing data [60]. In [34], the authors used a data augmentation module in their supervised contrastive learning approach that achieved SOTA performance. Direct augmentation from time-series data to train the model was also previously used with the aim to improve the performance [61]. The issue with data augmentation is it requires separate computation to produce new samples with risks of noise inclusion, and ineffectiveness if the augmentation procedure is not carefully optimized. On the other hand, the weight assignment method is easier and is directly implemented with the cost function during training. In our study we had three choices of weight calculation for the cost function. First, the regular weight calculation which measures the number of samples in a class and calculates a weight inversely proportional to that number. However, the deviation of minimum weight to the maximum is very high. The regular weight calculation can potentially reduce the learning capability of samples with sufficient training data, as shown in Fig. 7. In section-II, we have described how we used the logarithmic scaling to reduce the variance and the deviation among the weights. Another choice of weight calculation is well known balanced weight calculation method inspired by [62]. The balanced weights are calculated as follows:  $w_m = \frac{N}{n_i \times C}$ , where,  $w_m$  denotes weight of  $m$ -th class,  $N$  indicates number of samples in the dataset,  $n_i$  is the number of samples in  $m^{\text{th}}$  class, and  $Y$  is the number of classes.

This method may produce weights with lower variance and deviation than the regular weight calculation. However, this

TABLE III

PERFORMANCE COMPARISON BETWEEN NEUROSLLEEPNET AND OTHER STATE-OF-THE-ART DEEP LEARNING BASED METHODS FOR AUTOMATIC SLEEP SCORING.

Database	Subjects	System			Overall Performance			Per-class F1 Score				
		Model	Input Type	S	Acc.	MF1	$\kappa$	W	N1	N2	N3	REM
Sleep-EDFx	78	<b>NeuroSleepNet</b>	<b>Raw signal</b>	<b>1</b>	<b>86.1</b>	<b>80.8</b>	<b>.805</b>	91.7	48.5	<b>89.3</b>	<b>88.7</b>	<b>84.6</b>
		SleePyCo [34]	Raw signal	10	84.6	79.0	0.787	<b>93.5</b>	50.4	86.5	80.5	84.2
		XSleepNet [38]	Raw Signal Spectrogram	20	84.0	77.9	0.778	--	--	--	--	--
		H. Korkalainen et. al.[30]	Raw signal	100	83.7	--	0.77	--	--	--	--	--
		TinySleepNet [29]	Raw Signal	15	83.1	78.1	0.77	92.8	<b>51.0</b>	85.3	81.1	80.3
		SeqSleepNet [25]	Spectrogram	20	82.6	76.4	0.760	--	--	--	--	--
		SleepTransformer [36]	Spectrogram	21	81.4	74.33	0.743	91.7	40.4	84.3	77.9	77.2
		U-Time [22]	Raw Signal	35	81.3	76.3	0.745	92.0	<b>51.0</b>	0.84	0.75	0.80
		AttnSleep [35]	Raw Signal	80	81.3	75.1	0.740	92.0	42.0	85.0	82.1	74.2
		SleepEEGNet [28]	Raw Signal	--	80.0	73.5	0.730	91.7	44.0	82.5	73.5	76.1
MESA	2,237	<b>NeuroSleepNet</b>	<b>Raw signal</b>	<b>1</b>	82.0	<b>76.3</b>	<b>0.753</b>	<b>91.6</b>	48.8	85.3	<b>80.0</b>	76.8
		FullSleepNet [31]	Raw Signal	Whole night	<b>90.8</b>	72.8	0.674	89.8	<b>52.2</b>	<b>85.5</b>	67.1	<b>86.1</b>
Physio2018	994	<b>NeuroSleepNet</b>	<b>Raw signal</b>	<b>1</b>	80.5	76.8	<b>0.738</b>	81.9	58.1	83.0	<b>81.5</b>	79.5
		SleePyCo [34]	Raw Signal	10	<b>80.9</b>	<b>78.9</b>	0.737	<b>84.2</b>	<b>59.3</b>	<b>85.3</b>	79.4	<b>86.3</b>
		XSleepNet [38]	Raw Signal Spectrogram	20	80.3	78.6	0.732	--	--	--	--	--
		SeqSleepNet [25]	Spectrogram	20	79.4	77.6	0.719	--	--	--	--	--
		U-Time [22]	Raw Signal	35	78.8	77.4	0.714	82.5	59.0	83.1	79.0	83.5
SHHS	5,791	<b>NeuroSleepNet</b>	<b>Raw signal</b>	<b>1</b>	86.7	<b>80.9</b>	0.804	85.5	<b>52.5</b>	<b>90.0</b>	<b>89.9</b>	86.6
		SleePyCo [34]	Raw signal	10	<b>87.9</b>	80.7	<b>0.830</b>	<b>92.6</b>	49.2	88.5	84.5	<b>88.6</b>
		SleepTransformer [36]	Spectrogram	21	87.7	80.1	.0828	92.2	46.1	88.3	85.2	<b>88.6</b>
		XSleepNet [38]	Raw Signal Spectrogram	20	87.6	80.7	0.826	92.0	49.9	88.3	85.0	88.2
		Sors et. al. [23]	Raw Signal	4(2 past)	86.8	78.5	0.85	91.4	42.7	88.0	84.9	85.4
		IITNET [41]	Raw Signal	10	86.7	79.8	0.812	90.1	48.1	88.4	85.2	87.2
		SeqSleepNet [25]	Spectrogram	20	86.5	78.5	0.81	--	--	--	--	--

method can also result in disproportionate penalization if one of the classes is very rare which is extremely likely for N1 class in sleep recording. The comparison of these three methods and without class weights is displayed in Fig. 6. The figure indicates slight deviations in per-class performance for W, N2, N3, and REM stages across no weights, regular weights, and balanced weights. However, our log scale-based weight assignment method outperforms all these techniques. While the improvement in N2 and REM stages is small, our weight assignment technique significantly enhances the W, N1 and N3 classes. If no weights are assigned, the loss function by default considers all equal weights of 1, resulting in a variance of 0. This does not prioritize the minority class such as N1 during training. The weight variances for the Sleep-EDFx database are 24.68 for regular weights, 0.98 for balanced weights, and 0.44 for log-scaled weights. Here, the variance of weights assigned by regular weight assignment are very high since they were inversely proportional to the number of samples. Thus, we can observe some improvement minority class such as N1. The balanced weights, in contrast, typically have lower variance than regular weights. We cannot argue that having lower variance improves the performance since most of the classes shows almost similar results. The variance of weights calculated by log scale is lower than both regular and balanced weights but higher than 0. Since, the log scale outperforms all of them, we assume that there may be an optimal variance of weights for which there will be improvement in performance

for minority class while having firm performance for classes with sufficient data.

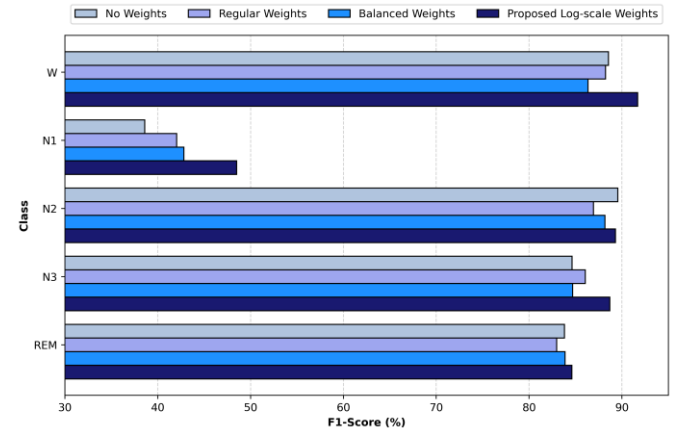


Fig.7: The per-class F1-scores for 5 different classes on three different weight assignment technique is compared. The log-scale based weight assignment technique provides higher per-class f1-score for all the classes indicating better and more balanced classification outcome.

### E. Univariate-NeuroSleepNet (Single channel without Spatial Convolution)

The results in tables III were calculated by applying multi-variate EEG signal. In this section, we discuss the modifications required to employ single channel EEG and its impact on the performance. In single channel implementation, the spatial convolution block becomes unnecessary since it was utilized to

learn cross-channel characteristics from multiple channels. The rest of the section remains same. In this part we evaluated our model using the Fpz-Cz and Pz-Cz channel individually on Sleep-EDFx. The results are displayed in Table IV. The results show that utilizing Fpz-Cz in our scheme does not reduce accuracy with respect to using two channels combined. The performance with Pz-Cz however is relatively lower than individual performance on Fpz-Cz. In previous baseline models, Fpz-Cz was used as their single channel framework and claimed that it achieves better results as single channel than Pz-Cz [16, 26] and [41].

TABLE IV  
PERFORMANCE OF THE NEUROSLLEEPNET MODEL WITH UNIVARIATE EEG INPUT

Ch. Name	Overall Performance			Per-Class F1-Score				
	Acc	MF1	$\kappa$	W	N1	N2	N3	REM
Fpz-Cz	83.4	77.4	0.771	87.5	42.0	88.6	88.2	80.7
Pz-Cz	82.3	76.0	0.756	88.7	37.4	87.6	86.2	80.0

#### F. Impact of Sequence Length (S)

Most of the previous automatic sleep scoring studies employed sequence lengths greater than one to achieve their SOTA performance. Meaningfully, a greater sequence length is vital for achieving better performance. In this section, we increase the input sequence length, S according to the design principle outlined in the 3<sup>rd</sup> statement of section II-A. The overall performance and per-class F1 scores are shown in Table V. The result shows the overall accuracy is almost similar to that of our one-to-one implementation. However, for sequence length of 5, there are slight improvement in accuracy, MF1 and Kappa value. The per-class F1-scores are also slightly higher for N2, N3 and REM class. However, for wake class the model performs better if the sequence length is reduced. These results show that even though our primary implementation accounts only single epoch, the performance for the increased sequence length with ours are pretty similar. Therefore, we claim that incorporation of RNN-based methods in the model to capture transitional changes that aligns with transition rules of AASM is no longer required. On the other hand, with increasing epoch length, the computational requirement also increases which is less of a concern in our case. We argue that one-to-one approaches are more viable medically and for real-time automatic sleep scoring implementation. However previous models with RNN tends to work better if sequence length is higher [26] [41]. Since a self-attention is RNN-free architecture, the same requirements can be fulfilled with the inclusion of positional encoding as used in [34] A future study will explore the performance of positional encoding with longer sequence lengths using NeuroSleepNet.

TABLE V  
PERFORMANCE COMPARISON OF NEUROSLLEEPNET MODEL WITH DIFFERENT SEQUENCE LENGTHS OF INPUT SIGNALS

S	Overall Performance			Per-Class F1-Score				
	Acc	MF1	$\kappa$	W	N1	N2	N3	REM
2	85.4	80.4	0.80	<b>89.1</b>	49.6	88.8	88.4	86.2
3	86.0	82.4	0.80	88.4	<b>57.4</b>	88.8	87.9	<b>89.4</b>

4	84.2	79.7	0.78	86.3	50.4	87.4	87.2	87.2
5	<b>87.0</b>	<b>82.9</b>	<b>0.82</b>	86.6	56.1	<b>89.0</b>	<b>90.0</b>	88.6

#### G. Impact of transforming convolutional features into contextual features

The main motivation for converting features extracted from the MTCL block into a contextual form was to strengthen the understanding of the shared characteristics among the stages. For example, although alpha wave (8-12) Hz is dominant in wake class, it is also observed partially in N2 class during sleep spindles and K-complexes. Conversely, the REM signal displays frequency characteristics of alpha (8-12 Hz), theta (4-8 Hz), and occasionally beta (12-30 Hz) waves, resembling the N1 wave, which primarily consists of theta waves with few alpha waves (less than 50%). The mix frequency characteristics make it harder for a low-capacity network to learn to differentiate between these waves effectively. In a transformer network, the encoder part can capture the meaning of each feature sequence ( $d_h$ ) in relation to its context within the temporal sequence ( $d_w$ ). The Multi-Head Self-Attention mechanism in a Transformer Encoder takes the regular extracted features and uses information from all the features in the sequence to update the feature sequences. Thus, the similarity in various convolutional features of different sleep waves becomes distinct, despite their similar frequency characteristics. Without the multi-head self-attention encoder in NeuroSleepNet, we examined that the rest of the model which provides accuracy 79.1%, mF1: 73.8 and Kappa score of 0.708 on Sleep-EDFx dataset. In comparison to the overall performance shown in Table III, the architecture with the encoder network improves accuracy by 7.0%, mF1 score by 7.7%, and kappa score by 0.097. The improvement in results indicates that the encoder network in NeuroSleepNet increases the capability of features significantly for distinguishing sleep stages.

## V. CONCLUSION

We introduced NeuroSleepNet, a novel automatic sleep scoring architecture based on EEG that utilizes a spatial and multi-scale temporal context learning feature extractor and a multi-head self-attention transformer encoder to convert static features into contextual representations. Our spatial learning helps to learn cross-channel characteristics by creating virtual channels and the MTCL learns the temporal context within the virtual channels with multiple temporal scales simultaneously. We also proposed a simplified scheme to incorporate transformer encoder to the representation learning. The spatial learning reduces the computational complexity for the following layers. We also modified the loss function with log-scaled weight assignment technique to have a more balanced performance. NeuroSleepNet provides comparable performances with the current SOTA architecture by using only single input epoch and excluded the requirement of transition rules. The model accommodates both univariate and multivariate inputs. We also compared the performance of single input sequence with multiple input sequences and showed that NeuroSleepNet provides almost similar performance on both cases. Our model also shows improved performance between N1 and REM stage.

We believe that NeuroSleepNet is a better approach for automatic sleep scoring for real-time implementation. As a natural extension of this work, we plan to apply NeuroSleepNet architecture for physiological signals extracted from wearables for monitoring sleep stages and sleep related disorders.

#### REFERENCES

- [1] A. D. Laposky, J. Bass, A. Kohsaka, and F. W. Turek, "Sleep and circadian rhythms: key components in the regulation of energy metabolism," *FEBS letters*, vol. 582, no. 1, pp. 142-151, 2008.
- [2] K. Wulff, S. Gatti, J. G. Wettstein, and R. G. Foster, "Sleep and circadian rhythm disruption in psychiatric and neurodegenerative disease," *Nature Reviews Neuroscience*, vol. 11, no. 8, pp. 589-599, 2010.
- [3] A. Rechtschaffen, "A manual of standardized terminology, techniques and scoring system for sleep stages of human subjects, pp. 1-55, 1968.
- [4] R. B. Berry, R. Brooks, C. E. Gamaldo, S. M. Harding, C. Marcus, and B. V. Vaughn, "The AASM manual for the scoring of sleep and associated events," *Rules, Terminology and Technical Specifications, Darien, Illinois, American Academy of Sleep Medicine*, vol. 176, no. 2012, pp. 7, 2012.
- [5] A. Malhotra, M. Younes, S. T. Kuna, R. Benca, C. A. Kushida, J. Walsh, A. Hanlon, B. Staley, A. I. Pack, and G. W. Pien, "Performance of an automated polysomnography scoring system versus computer-assisted manual scoring," *Sleep*, vol. 36, no. 4, pp. 573-582, 2013.
- [6] E. E. Schadt, M. D. Linderman, J. Sorenson, L. Lee, and G. P. Nolan, "Computational solutions to large-scale data management and analysis," *Nature reviews genetics*, vol. 11, no. 9, pp. 647-657, 2010.
- [7] H. Sun, J. Jia, B. Goparaju, G.-B. Huang, O. Sourina, M. T. Bianchi, and M. B. Westover, "Large-scale automated sleep staging," *Sleep*, vol. 40, no. 10, pp. zsx139, 2017.
- [8] K. A. I. Aboalayon, M. Faezipour, W. S. Almuhammadi, and S. Moslehpour, "Sleep stage classification using EEG signal analysis: a comprehensive survey and new investigation," *Entropy*, vol. 18, no. 9, pp. 272, 2016.
- [9] C. Berthomier, X. Drouot, M. Herman-Stoica, P. Berthomier, J. Prado, D. Bokar-Thire, O. Benoit, J. Mattout, and M.-P. d'Ortho, "Automatic analysis of single-channel sleep EEG: validation in healthy individuals," *Sleep*, vol. 30, no. 11, pp. 1587-1595, 2007.
- [10] B. Koley, and D. Dey, "An ensemble system for automatic sleep stage classification using single channel EEG signal," *Computers in biology and medicine*, vol. 42, no. 12, pp. 1186-1195, 2012.
- [11] X. Li, L. Cui, S. Tao, J. Chen, X. Zhang, and G.-Q. Zhang, "Hyclasss: a hybrid classifier for automatic sleep stage scoring," *IEEE journal of biomedical and health informatics*, vol. 22, no. 2, pp. 375-385, 2017.
- [12] L. Fraiwan, K. Lweesy, N. Khasawneh, H. Wenz, and H. Dickhaus, "Automated sleep stage identification system based on time-frequency analysis of a single EEG channel and random forest classifier," *Computer methods and programs in biomedicine*, vol. 108, no. 1, pp. 10-19, 2012.
- [13] D. Wulsin, J. Gupta, R. Mani, J. Blanco, and B. Litt, "Modeling electroencephalography waveforms with semi-supervised deep belief nets: fast classification and anomaly measurement," *Journal of neural engineering*, vol. 8, no. 3, pp. 036015, 2011.
- [14] F. Ebrahimi, M. Mikaeili, E. Estrada, and H. Nazeran, "Automatic sleep stage classification based on EEG signals by using neural networks and wavelet packet coefficients." pp. 1151-1154.
- [15] V. P. Jain, V. Mytri, V. Shete, and B. Shiragapur, "Sleep stages classification using wavelettransform & neural network." pp. 71-74.
- [16] O. Tsinalis, P. M. Matthews, and Y. Guo, "Automatic sleep stage scoring using time-frequency analysis and stacked sparse autoencoders," *Annals of biomedical engineering*, vol. 44, pp. 1587-1597, 2016.
- [17] N. Michielli, U. R. Acharya, and F. Molinari, "Cascaded LSTM recurrent neural network for automated sleep stage classification using single-channel EEG signals," *Computers in biology and medicine*, vol. 106, pp. 71-81, 2019.
- [18] Y. Zhang, Z. Yang, K. Lan, X. Liu, Z. Zhang, P. Li, D. Cao, J. Zheng, and J. Pan, "Sleep stage classification using bidirectional lstm in wearable multi-sensor systems." pp. 443-448.
- [19] M. Långkvist, L. Karlsson, and A. Loutfi, "Sleep stage classification using unsupervised feature learning," *Advances in Artificial Neural Systems*, vol. 2012, no. 1, pp. 107046, 2012.
- [20] J. B. Stephansen, A. N. Olesen, M. Olsen, A. Ambati, E. B. Leary, H. E. Moore, O. Carrillo, L. Lin, F. Han, and H. Yan, "Neural network analysis of sleep stages enables efficient diagnosis of narcolepsy," *Nature communications*, vol. 9, no. 1, pp. 5229, 2018.
- [21] H. Phan, F. Andreotti, N. Cooray, O. Y. Chén, and M. De Vos, "Automatic sleep stage classification using single-channel eeg: Learning sequential features with attention-based recurrent neural networks." pp. 1452-1455.
- [22] M. Perslev, M. Jensen, S. Darkner, P. J. Jennum, and C. Igel, "U-time: A fully convolutional network for time series segmentation applied to sleep staging," *Advances in Neural Information Processing Systems*, vol. 32, 2019.
- [23] A. Sors, S. Bonnet, S. Mirek, L. Vercueil, and J.-F. Payen, "A convolutional neural network for sleep stage scoring from raw single-channel EEG," *Biomedical Signal Processing and Control*, vol. 42, pp. 107-114, 2018.
- [24] H. Dong, A. Supratak, W. Pan, C. Wu, P. M. Matthews, and Y. Guo, "Mixed neural network approach for temporal sleep stage classification," *IEEE Transactions on Neural Systems and Rehabilitation Engineering*, vol. 26, no. 2, pp. 324-333, 2017.
- [25] H. Phan, F. Andreotti, N. Cooray, O. Y. Chén, and M. De Vos, "SeqSleepNet: end-to-end hierarchical recurrent neural network for sequence-to-sequence automatic sleep staging," *IEEE Transactions on Neural Systems and Rehabilitation Engineering*, vol. 27, no. 3, pp. 400-410, 2019.
- [26] A. Supratak, H. Dong, C. Wu, and Y. Guo, "DeepSleepNet: A model for automatic sleep stage scoring based on raw single-channel EEG," *IEEE transactions on neural systems and rehabilitation engineering*, vol. 25, no. 11, pp. 1998-2008, 2017.
- [27] L. Zhuang, M. Dai, Y. Zhou, and L. Sun, "Intelligent automatic sleep staging model based on CNN and LSTM," *Frontiers in Public Health*, vol. 10, pp. 946833, 2022.
- [28] S. Mousavi, F. Afghah, and U. R. Acharya, "SleepEEGNet: Automated sleep stage scoring with sequence to sequence deep learning approach," *PLoS one*, vol. 14, no. 5, pp. e0216456, 2019.
- [29] A. Supratak, and Y. Guo, "TinySleepNet: An efficient deep learning model for sleep stage scoring based on raw single-channel EEG." pp. 641-644.
- [30] H. Korkalainen, J. Aakko, S. Nikkonen, S. Kainulainen, A. Leino, B. Duce, I. O. Afara, S. Myllymaa, J. Töyräs, and T. Leppänen, "Accurate deep learning-based sleep staging in a clinical population with suspected obstructive sleep apnea," *IEEE journal of biomedical and health informatics*, vol. 24, no. 7, pp. 2073-2081, 2019.
- [31] H. Zan, and A. Yildiz, "Multi-task learning for arousal and sleep stage detection using fully convolutional networks," *Journal of Neural Engineering*, vol. 20, no. 5, pp. 056034, 2023.
- [32] W. Qu, Z. Wang, H. Hong, Z. Chi, D. D. Feng, R. Grunstein, and C. Gordon, "A residual based attention model for EEG based sleep staging," *IEEE journal of biomedical and health informatics*, vol. 24, no. 10, pp. 2833-2843, 2020.
- [33] Y. Dai, X. Li, S. Liang, L. Wang, Q. Duan, H. Yang, C. Zhang, X. Chen, L. Li, and X. Li, "Multichannelsleepnet: A transformer-based model for automatic sleep stage classification with psg," *IEEE Journal of Biomedical and Health Informatics*, vol. 27, no. 9, pp. 4204-4215, 2023.
- [34] S. Lee, Y. Yu, S. Back, H. Seo, and K. Lee, "Sleepyco: Automatic sleep scoring with feature pyramid and contrastive learning," *Expert Systems with Applications*, vol. 240, pp. 122551, 2024.
- [35] E. Eldele, Z. Chen, C. Liu, M. Wu, C.-K. Kwok, X. Li, and C. Guan, "An attention-based deep learning approach for sleep stage classification with single-channel EEG," *IEEE Transactions on Neural Systems and Rehabilitation Engineering*, vol. 29, pp. 809-818, 2021.
- [36] H. Phan, K. Mikkelsen, O. Y. Chén, P. Koch, A. Mertins, and M. De Vos, "Sleeptransformer: Automatic sleep staging with interpretability and uncertainty quantification," *IEEE Transactions on Biomedical Engineering*, vol. 69, no. 8, pp. 2456-2467, 2022.

- [37] H. Phan, F. Andreotti, N. Cooray, O. Y. Chén, and M. De Vos, "Joint classification and prediction CNN framework for automatic sleep stage classification," *IEEE Transactions on Biomedical Engineering*, vol. 66, no. 5, pp. 1285-1296, 2018.
- [38] H. Phan, O. Y. Chén, M. C. Tran, P. Koch, A. Mertins, and M. De Vos, "XSleepNet: Multi-view sequential model for automatic sleep staging," *IEEE Transactions on Pattern Analysis and Machine Intelligence*, vol. 44, no. 9, pp. 5903-5915, 2021.
- [39] A. Vilamala, K. H. Madsen, and L. K. Hansen, "Deep convolutional neural networks for interpretable analysis of EEG sleep stage scoring," pp. 1-6.
- [40] P. Jadhav, G. Rajguru, D. Datta, and S. Mukhopadhyay, "Automatic sleep stage classification using time-frequency images of CWT and transfer learning using convolution neural network," *Biocybernetics and Biomedical Engineering*, vol. 40, no. 1, pp. 494-504, 2020.
- [41] H. Seo, S. Back, S. Lee, D. Park, T. Kim, and K. Lee, "Intra- and inter-epoch temporal context network (IITNet) using sub-epoch features for automatic sleep scoring on raw single-channel EEG," *Biomedical signal processing and control*, vol. 61, pp. 102037, 2020.
- [42] C. Sun, C. Chen, W. Li, J. Fan, and W. Chen, "A hierarchical neural network for sleep stage classification based on comprehensive feature learning and multi-flow sequence learning," *IEEE journal of biomedical and health informatics*, vol. 24, no. 5, pp. 1351-1366, 2019.
- [43] M. X. Cohen, *Analyzing neural time series data: theory and practice*: MIT press, 2014.
- [44] L. Fiorillo, P. Favaro, and F. D. Faraci, "Deepsleepnet-lite: A simplified automatic sleep stage scoring model with uncertainty estimates," *IEEE transactions on neural systems and rehabilitation engineering*, vol. 29, pp. 2076-2085, 2021.
- [45] J. Huang, L. Ren, X. Zhou, and K. Yan, "An improved neural network based on SENet for sleep stage classification," *IEEE Journal of Biomedical and Health Informatics*, vol. 26, no. 10, pp. 4948-4956, 2022.
- [46] B. Blankertz, R. Tomioka, S. Lemm, M. Kawanabe, and K.-R. Muller, "Optimizing spatial filters for robust EEG single-trial analysis," *IEEE Signal processing magazine*, vol. 25, no. 1, pp. 41-56, 2007.
- [47] M. Z. Baig, N. Aslam, and H. P. Shum, "Filtering techniques for channel selection in motor imagery EEG applications: a survey," *Artificial intelligence review*, vol. 53, no. 2, pp. 1207-1232, 2020.
- [48] V. J. Lawhern, A. J. Solon, N. R. Waytowich, S. M. Gordon, C. P. Hung, and B. J. Lance, "EEGNet: a compact convolutional neural network for EEG-based brain-computer interfaces," *Journal of neural engineering*, vol. 15, no. 5, pp. 056013, 2018.
- [49] S. Stober, A. Stermin, A. M. Owen, and J. A. Grahn, "Deep feature learning for EEG recordings," *arXiv preprint arXiv:1511.04306*, 2015.
- [50] S. Chambon, M. N. Galtier, P. J. Arnal, G. Wainrib, and A. Gramfort, "A deep learning architecture for temporal sleep stage classification using multivariate and multimodal time series," *IEEE Transactions on Neural Systems and Rehabilitation Engineering*, vol. 26, no. 4, pp. 758-769, 2018.
- [51] A. Vaswani, N. Shazeer, N. Parmar, J. Uszkoreit, L. Jones, A. N. Gomez, Ł. Kaiser, and I. Polosukhin, "Attention is all you need," *Advances in neural information processing systems*, vol. 30, 2017.
- [52] B. Kemp, A. H. Zwinderman, B. Tuk, H. A. Kamphuisen, and J. J. Obery, "Analysis of a sleep-dependent neuronal feedback loop: the slow-wave microcontinuity of the EEG," *IEEE Transactions on Biomedical Engineering*, vol. 47, no. 9, pp. 1185-1194, 2000.
- [53] M. Mourtazaev, B. Kemp, A. Zwinderman, and H. Kamphuisen, "Age and gender affect different characteristics of slow waves in the sleep EEG," *Sleep*, vol. 18, no. 7, pp. 557-564, 1995.
- [54] A. L. Goldberger, L. A. Amaral, L. Glass, J. M. Hausdorff, P. C. Ivanov, R. G. Mark, J. E. Mietus, G. B. Moody, C.-K. Peng, and H. E. Stanley, "PhysioBank, PhysioToolkit, and PhysioNet: components of a new research resource for complex physiologic signals," *circulation*, vol. 101, no. 23, pp. e215-e220, 2000.
- [55] G.-Q. Zhang, L. Cui, R. Mueller, S. Tao, M. Kim, M. Rueschman, S. Mariani, D. Mobley, and S. Redline, "The National Sleep Research Resource: towards a sleep data commons," *Journal of the American Medical Informatics Association*, vol. 25, no. 10, pp. 1351-1358, 2018.
- [56] X. Chen, R. Wang, P. Zee, P. L. Lutsey, S. Javaheri, C. Alcántara, C. L. Jackson, M. A. Williams, and S. Redline, "Racial/ethnic differences in sleep disturbances: the Multi-Ethnic Study of Atherosclerosis (MESA)," *Sleep*, vol. 38, no. 6, pp. 877-888, 2015.
- [57] S. F. Quan, B. V. Howard, C. Iber, J. P. Kiley, F. J. Nieto, G. T. O'Connor, D. M. Rapoport, S. Redline, J. Robbins, and J. M. Samet, "The sleep heart health study: design, rationale, and methods," *Sleep*, vol. 20, no. 12, pp. 1077-1085, 1997.
- [58] M. M. Ghassemi, B. E. Moody, L.-W. H. Lehman, C. Song, Q. Li, H. Sun, R. G. Mark, M. B. Westover, and G. D. Clifford, "You snooze, you win: the physionet/computing in cardiology challenge 2018," pp. 1-4.
- [59] J. S. Barlow, "Electroencephalography: basic principles, clinical applications and related fields," *JAMA*, vol. 250, no. 22, pp. 3108-3108, 1983.
- [60] G. Iglesias, E. Talavera, Á. González-Prieto, A. Mozo, and S. Gómez-Canaval, "Data augmentation techniques in time series domain: a survey and taxonomy," *Neural Computing and Applications*, vol. 35, no. 14, pp. 10123-10145, 2023.
- [61] C. Sun, J. Fan, C. Chen, W. Li, and W. Chen, "A two-stage neural network for sleep stage classification based on feature learning, sequence learning, and data augmentation," *IEEE Access*, vol. 7, pp. 109386-109397, 2019.
- [62] G. King, and L. Zeng, "Logistic regression in rare events data," *Political analysis*, vol. 9, no. 2, pp. 137-163, 2001.